

# Supporting Information

to the paper

## Ni(II), Co(II), Cu(II), Zn(II) and Na(I) complexes of a hybrid ligand 4'-(4'''-benzo-15-crown-5)-methoxy-2,2':6',2''-terpyridine

Nadezhda M. Logacheva,<sup>a</sup> Vladimir E. Baulin,<sup>a</sup> Aslan Yu. Tsivadze,<sup>a</sup> Elena N. Pyatova,<sup>b</sup> Irina S. Ivanova<sup>b</sup>, Yurii A. Velikodny<sup>c</sup> and Vladimir V. Chernyshev<sup>a, c\*</sup>

<sup>a</sup>A. N. Frumkin Institute of Physical Chemistry and Electrochemistry, Leninsky prospect 31, 119991 Moscow GSP-1, Russian Federation,

<sup>b</sup>N.S. Kurnakov Institute of General and Inorganic Chemistry, Leninsky prospect 31, 119991 Moscow GSP-1, Russian Federation

<sup>c</sup>Department of Chemistry, Moscow State University, 119991 Moscow, Russian Federation

Correspondence e-mail: vladimir@struct.chem.msu.ru

### Table of contents

<b>Part 1.</b>	
IR-spectroscopy	S1
Tables	S7
IR-spectra for <i>L</i> and <b>1-10</b> .	S11
<b>Part 2.</b>	
X-ray crystallography. Figures.	S22

# PART 1

## IR-spectroscopy

IR spectra were recorded as Nujol mulls on a Bruker Vertex 70 spectrophotometer in the range 4000–400  $\text{cm}^{-1}$  (suspensions in liquid paraffin, KBr plates).

The bands in the IR spectrum of L in the range 1700–400  $\text{cm}^{-1}$  were assigned on the basis of comparison of the vibrational spectra of 4'-chloroterpyridine (CTP), 4'-hydroxymethylbenzo-15-crown-5 (HMB15C5), and benzo-15-crown-5 (B15C5) and the data on pyridine<sup>1,2</sup>. Selected vibrational frequencies in the IR spectra of L and its complexes are summarized in Table 1.

As compared with the spectra of CTP and HMB15C5, the IR spectrum of L shows two new strong narrow bands at 1352 and 1197  $\text{cm}^{-1}$ ; they can be assigned to vibrations of a new moiety Ph–H<sub>2</sub>C–O–Py, which resulted from the attachment of CTP to HMB15C5. This moiety is analogous to the Ph–O–CH<sub>2</sub> moiety of B15C5. However, the  $\nu(\text{PyO})$  and  $\nu(\text{CO})$  frequencies for the former are somewhat higher than the corresponding frequencies in the spectrum of B15C5, which is presumably due to its position between two aromatic rings. There are no ways to concretely identify what bond is responsible for a certain band since the bonds are strongly conjugated due to the aromaticity of the system.

The spectra of crown ethers in the range 1150–1050  $\text{cm}^{-1}$  show  $\nu_{\text{as}}(\text{COC})$  and  $\nu_{\text{s}}(\text{COC})$  vibration bands. The IR spectrum of L in this range shows two bands: the strong band at 1144  $\text{cm}^{-1}$  and the medium band at 1119  $\text{cm}^{-1}$ . According to the correlations in<sup>3,4</sup>, for benzocrown ethers and their azomethine derivatives, a frequency of  $\sim 1120 \text{ cm}^{-1}$  is due to the  $\nu_{\text{as}}(\text{COC})$  vibration of an ethylene glycol unit with a conformation close to TGG. The band at 1144  $\text{cm}^{-1}$  arises, most likely, from the  $\delta(\text{CH})_{\text{Ph}}$  bending vibrations.

However, most information on the conformational structure of B15C5 is extracted from the spectral region 1000–700  $\text{cm}^{-1}$  where the breathing vibration  $\nu_{\text{resp}}$  of the macrocycle and composite stretching–bending vibrations  $\rho(\text{CH}_2) + \nu(\text{CO}) + \nu(\text{CC})$  of separate ethylene glycol units are observed<sup>5</sup>. Inasmuch as the IR spectrum of CTP shows only two bands in the range 993–780  $\text{cm}^{-1}$  (882 and 816  $\text{cm}^{-1}$ ), we can suggest the conformational structure of the macrocycle in free L.

Previously<sup>3</sup>, the conformations of B15C5 and its complexes were studied by vibrational spectroscopy. It was shown in<sup>4</sup> that the introduction of different substituents into the benzene ring of B15C5 leads to a change in the conformation of the macrocycle and deviation of torsion angles from their ideal values (180° for T, 120° for S, 60° for G, and 180° for C). Based on X-ray crystallographic<sup>6–9</sup> and spectral data<sup>4,10,11</sup>, a relationship between the frequency and conformation of the ethylene glycol unit was studied for some azomethine derivatives of B15C5 and nitrobenzo-

15C5 and their complexes. Here, we used these results as a basis for speculation about the conformation of the macrocycle in the uncoordinated L.

In particular, according to<sup>3,4</sup>, the band at 932 cm<sup>-1</sup> in the spectrum of L can be assigned to the moiety composed of two TGT and TGG units, the weak band at 953 cm<sup>-1</sup> can be due to the TGT unit, and the band at 920 cm<sup>-1</sup> can be assigned to the vibration of a unit with a conformation close to TGG. The doublet comprising the medium band at 855 cm<sup>-1</sup> and the weaker band at 845 cm<sup>-1</sup> can be assigned to the vibration of the TGT unit. The bands at 870 and 829 cm<sup>-1</sup> are presumably due to vibrations of a unit with the conformation close to TGS. The band at 766 cm<sup>-1</sup> can be assigned to the macrocycle-breathing vibration  $\nu_{\text{resp}}$ . Thus, we can assume that the macrocycle conformation in the molecule of free L is described by the formula TCT TGT TGG TGS TGT.

The IR spectrum of the complex [NaNCS•L] (**6**) differs from the spectrum of free L in conformationally sensitive regions. At the same time, the positions of the  $\nu_{\text{Ph}}$ ,  $\nu_{\text{Py}}$ , and  $\nu(\text{PyO}) + \nu(\text{CO})$  bands, as well as the bending vibrations of CTP angles, remain almost the same, which is evidence that the heterocyclic nitrogen atoms are not involved in coordination.

The breathing vibration frequency (766 cm<sup>-1</sup> for L) increases to 865 cm<sup>-1</sup> in the spectrum of the sodium complex, which is typical of the maxidentate conformation of the macrocycle in the complex. The coordination of B15C5 through the anisole oxygen atoms is supported by a decrease in the  $\nu_{\text{as}}(\text{PhO})$  frequency by 24 cm<sup>-1</sup> (1250 and 1226 cm<sup>-1</sup> in L and **6**, respectively).

According to X-ray diffraction evidence, the macrocycle of B15C5 in this complex is composed of four TGT units and a closing TCT unit and has symmetry  $C_s$ . In agreement with this structure, the IR spectrum of the sodium complex **6** shows in the range 1100–800 cm<sup>-1</sup> the bands typical of the TGT system at 1101, 968, 943, and 835 cm<sup>-1</sup>. The TCT unit has no vibrations in this frequency range.

The coordinated NCS<sup>-</sup> group in the complex gives rise to the doublet band with maxima at 2056 and 2046 cm<sup>-1</sup>, which is somewhat lower than the expected value.

The coordination of L to transition metals through the heterocyclic nitrogen atoms of the terpyridine moiety also leads to certain changes in its IR spectrum.

It is worth noting that the vibrational spectra of all synthesized complexes with transition metals (**1-5**) are analogous, except the regions of conformationally sensitive stretching–bending vibrations of the macrocycle (975–800 cm<sup>-1</sup>). As distinct from the spectra of transition metal complexes, many bands in the spectrum of the copper complex **3** are split.

A change in the conformationally sensitive region of spectra is quite natural since, as shown by X-ray crystallography, the macrocycle of the B15C5 ligand has different conformations in the complexes:

[NaNCS•L] ( <b>6</b> )	T.CT. TGT. TG.T. TG.T T.GT
[CoL <sub>2</sub> ](NCS) <sub>2</sub> ( <b>5</b> )	a) TCT SGT. S <sub>+</sub> ST GGT GGT <sub>+</sub> b) TCT T.ST <sub>+</sub> S.S.T G <sub>+</sub> GG TGS <sub>+</sub>
[CoL <sub>2</sub> ](PF <sub>6</sub> ) <sub>2</sub> •3H <sub>2</sub> O ( <b>2</b> )	T.CT T.G <sub>+</sub> T G <sub>+</sub> G <sub>+</sub> T GG T TGT
[NiL <sub>2</sub> ](PF <sub>6</sub> ) <sub>2</sub> •2(C <sub>2</sub> H <sub>5</sub> OH)•H <sub>2</sub> O ( <b>1</b> )	TCT T.GT S.G <sub>+</sub> T G <sub>+</sub> G.T TGT
[ZnL <sub>2</sub> ](PF <sub>6</sub> ) <sub>2</sub> •3H <sub>2</sub> O ( <b>4</b> )	T.CT. T.GT. T.GG <sub>+</sub> T.G <sub>+</sub> S S <sub>+</sub> GT
[CuL <sub>2</sub> ](PF <sub>6</sub> ) <sub>2</sub> ( <b>3</b> )	a) TCT. SG <sub>+</sub> G <sub>+</sub> S.S <sub>+</sub> G <sub>+</sub> S <sub>+</sub> C <sub>+</sub> S T.GT b) TCT TGS. S.SS. G <sub>+</sub> GS TGT

The  $\nu_{\text{Py}}$  vibration of terpyridine and the  $\nu_{\text{Ph}}$  vibration of benzocrown ether are observed in the range 1622–1514  $\text{cm}^{-1}$  (Table 1). Among these bands, the lowest frequency band is presumably due to vibrations of the benzene ring in the crown ether ( $\nu_{\text{Ph}}$ ); it is slightly shifted to a low-frequency region (7–10  $\text{cm}^{-1}$ ) as compared to its position in the spectrum of the free ligand. The other frequencies in the spectra of all complexes, which were assigned to mainly stretching vibrations of heterocycles, are higher as compared with analogous frequencies for the free ligand. Such an increase in  $\nu_{\text{Py}}$  caused by coordination is in agreement with the evidence<sup>12</sup> that the coordination of nicotinamide through the nitrogen atom leads to an increase in  $\nu_{\text{Py}}$ .

The bands due to the  $\nu_{\text{s}}(\text{PhO})$  and  $\nu_{\text{as}}(\text{PhO})$  vibrations of the crown ether moiety of the L molecule retain their positions upon coordination, which confirms the fact that the anisole oxygen atoms are not involved in coordination.

In the IR spectra of the complexes **1-5**, the band at 1197  $\text{cm}^{-1}$ , assigned to  $\nu(\text{Py-O}) + \nu(\text{CO})$ , is shifted by 8–10  $\text{cm}^{-1}$  toward higher frequencies as compared with its position in the spectrum of the free ligand L. Inasmuch as this vibration is observed as a narrow strong band in the spectra of L and its complexes, it can be used as analytical for determination of the coordination of L through the heterocyclic nitrogen atoms.

Some changes caused by complexation are also observed in the  $\nu_{\text{as}}(\text{COC})$  and  $\nu_{\text{s}}(\text{COC})$  region. The IR spectrum of the uncoordinated L shows two bands at 1143 and 1119  $\text{cm}^{-1}$  in this region, whereas the spectrum of the zinc complex **4** shows a strong band at 1138  $\text{cm}^{-1}$ , two weak bands at 1119 and 1112  $\text{cm}^{-1}$ , and a medium band at 1099  $\text{cm}^{-1}$ . Based on the structural data and our correlations, the bands at 1119, 1112, and 1099  $\text{cm}^{-1}$  can be assigned to the T.GG<sub>+</sub>, TGS, and T.GT unit vibrations, respectively.

In a lower frequency range of 950–800  $\text{cm}^{-1}$ , the spectra of all hexafluorophosphate complexes **1-4** show a broad strong band at 845–833  $\text{cm}^{-1}$  caused by stretching vibrations of the  $\text{PF}_6^-$  anion, which overlaps most of the stretching–bending vibration bands of the macrocycle. Nevertheless, the spectrum of the zinc complex **4** shows a medium band at 933  $\text{cm}^{-1}$  (932  $\text{cm}^{-1}$  in

the spectrum of L), which can be assigned to the TGT TGG moiety. A weak band at  $910\text{ cm}^{-1}$  is presumably due to the TGG unit.

The  $\delta(\text{PF}_6)$  bending vibrations in the spectra of all complexes are observed as a narrow strong band at  $558\text{--}555\text{ cm}^{-1}$ .

The well-resolved bands at  $3637$ ,  $3535$ , and  $3435\text{ cm}^{-1}$  in the spectrum of the complex (Table 1) correspond to the stretching vibrations of the outer-sphere water.

The IR spectrum of the nickel complex **1** is analogous to that of the zinc complex **4** in the entire spectral range, including the conformationally sensitive regions. In particular, the spectrum of the nickel complex also shows in the  $\nu_{\text{as}}(\text{COC})$  region three bands at  $1118$ ,  $1111$ , and  $1100\text{ cm}^{-1}$ , which we assigned to the TGG, TGS, and TGT ethylene glycol units, respectively. The other conformationally sensitive region shows the band at  $936\text{ cm}^{-1}$  due to the TGT TGG moiety and the band at  $921\text{ cm}^{-1}$  caused, in our opinion, by the TGG unit.

The spectrum of the cobalt hexafluorophosphate complex **2** is somewhat different from the spectra of the above complexes: it is smoother, which can be evidence of the polymeric structure of this complex. According to X-ray crystallographic data, the macrocycle of the ligand in this complex is conformationally more homogeneous. The IR spectrum of the complex is consistent with the structural data: only the bands due to the TGT and TGG ethylene glycol units are observed, namely, at  $1103$  and  $1095\text{ cm}^{-1}$  for TGT,  $904\text{ cm}^{-1}$  for TGG, and  $937\text{ cm}^{-1}$  for the TGT TGG moiety.

As mentioned above, more significant differences are observed in the IR spectrum of the copper hexafluorophosphate complex **3**. The general pattern persists, although many bands are split. This fact can be evidence either that the macrocycles in the complex have different conformations, or that each of the macrocycles is conformationally inhomogeneous, or that the corresponding crystal structures are different. According to X-ray crystallography evidence, all three factors are involved. A similar situation was observed for the inner complex copper salt  $\text{CuL}_2'$  with an azomethine derivative of B15C5 (L' is 4'-[2-(tosylamino)benzylideneamino]-2,3-benzo-15-crown-5<sup>10</sup>). X-ray crystallography showed that the two macrocycles incorporated in the compound have different conformations as distinct from the zinc salt of the same composition.

In the  $\nu_{\text{as}}(\text{COC})$  region, the spectrum of the copper hexafluorophosphate complex **3** shows three bands: the strong band at  $1128\text{ cm}^{-1}$  presumably due the SGG unit, the medium band at  $1112\text{ cm}^{-1}$  corresponding to the TGS unit, and the weak band at  $1095\text{ cm}^{-1}$  caused by the presence of the TGT unit. In the range  $950\text{--}800\text{ cm}^{-1}$ , the spectrum shows a new medium band as compared with the spectrum of the free ligand L and the other hexafluorophosphate complexes **1**, **2** and **4**. It can be tentatively assigned to the unit with a conformation other than those mentioned above, namely, to the S.S<sub>+</sub>G<sub>+</sub> or S.SS. unit.

In contrast to the other complexes, the copper complex **3** does not contain water molecules, which is also responsible for a different crystal structure and, hence, for the difference of its spectrum from the spectra of the other complexes.

Structural study of  $[\text{CoL}_2](\text{NCS})_2$  (**5**) revealed a significant difference between the structure of this complex and those of analogous hexafluorophosphate complexes. The spectrum of this compound is smoother, which can be caused by the presence of a considerable amount of an amorphous component. Therefore, despite considerable conformational inhomogeneity of each of the macrocycles, the spectrum shows only the bands typical of ethylene glycol units with TGG and TST conformations at 858 and 847  $\text{cm}^{-1}$  for TST and 935  $\text{cm}^{-1}$  for TST TGG.

The outer-sphere  $\text{NCS}^-$  group gives rise to the narrow strong band at 2047  $\text{cm}^{-1}$ .

In the IR spectra of all synthesized complexes, the bands corresponding to the NCC, CCC, and CNC bending vibrations of the terpyridine moiety are somewhat shifted toward higher frequencies as compared to their position in the spectrum of the free ligand L (Table 1), which also confirms the coordination of the complex-forming metal atom through the heterocyclic nitrogen atoms.

We found that, in  $[\text{CuL}_2 \cdot \text{NaNCS} \cdot \text{Na}(\text{NCS})_2] \text{NCS} \cdot \text{CH}_3\text{CN}$  (**11**), the copper cation is coordinated to the terpyridine moiety of the ligand L through three nitrogen atoms and each sodium cation is coordinated to the oxygen atoms of the crown ether ring. Inasmuch as the vibrational spectra of all trinuclear complexes are analogous, we can draw the conclusion that the transition and alkali metals in these compounds have the same coordination modes. The coordination of the ether oxygen atoms of the macrocycles by the sodium cations leads to changes mainly in the conformationally sensitive regions of vibrational spectra. Selected conformation-sensitive frequencies in the spectra of the trinuclear complexes are listed in Table 2.

The coordination of the anisole oxygen atoms by the sodium cations in all trinuclear complexes is reflected by a decrease in  $\nu_{\text{as}}(\text{PhO})$  by 17–26  $\text{cm}^{-1}$ . Comparison of the conformation-sensitive regions in the IR spectra of the trinuclear complexes **7–11** and  $[\text{NaNCS} \cdot \text{L}]$  (**6**) allows us to believe that the conformation of B15C5 in these complexes is close to its conformation in **6**. X-ray crystallography shows that the macrocycle in **6** is composed of four TGT units and a closing TCT unit and has symmetry  $C_s$ . The spectra of the trinuclear complexes also show the bands typical of the TGT system at 1100 and 937–941  $\text{cm}^{-1}$ .

The breathing vibration band of the macrocycle is observed at 860–870  $\text{cm}^{-1}$  and is likely overlapped by the strong band at 845  $\text{cm}^{-1}$  due to the  $\text{PF}_6^-$  anion.

According to X-ray crystallographic data on **11**, the four thiocyanato groups incorporated in the complex have different functions: three of them are coordinated to the sodium cations, and one group is an outer-sphere one. In agreement with this, the  $\nu(\text{CN})$  band at 2068  $\text{cm}^{-1}$  is due to the

coordinated thiocyanato groups and the  $\nu(\text{CN})$  band at  $2041\text{ cm}^{-1}$  arises from the outer-sphere  $\text{NCS}^-$  anion.

Table 1. Assignment of vibrational frequencies ( $\text{cm}^{-1}$ ) in the IR spectra of L and its complexes

Assignment	L	[ZnL <sub>2</sub> ](PF <sub>6</sub> ) <sub>2</sub> •3H <sub>2</sub> O (4)	[NiL <sub>2</sub> ](PF <sub>6</sub> ) <sub>2</sub> •2(C <sub>2</sub> H <sub>5</sub> OH) •H <sub>2</sub> O (1)	[CoL <sub>2</sub> ](PF <sub>6</sub> ) <sub>2</sub> •3H <sub>2</sub> O (2)	[CuL <sub>2</sub> ](PF <sub>6</sub> ) <sub>2</sub> (3)	[NaNCS•L] (6)	[CoL <sub>2</sub> ](NCS) <sub>2</sub> (5)
$\nu(\text{H}_2\text{O})$		3637 3535 3435	3637 3544 3446	3624  3468		3413	3380
$\nu_{\text{Ph}}, \nu_{\text{Py}}$	1600 1583 1564  1524	1614 1601 1574 1560 1517	1616 1602 1572 1560 1517	1614 1604 sh 1570 1558 1517	1622 1600 1575 1561 1557 1514	1598 1580 1560	1612 1599 1568  1556 1514
$\delta(\text{CH})_{\text{Py}},$ $\delta(\text{CH})_{\text{Ph}}$ $\delta(\text{CH}_2)$	1467 1464 1456 1444 1432  1405 1377	1477 1463 1457  1439	1474 1462 1455 1443 1439 1420  1377	 1463 1455 1444 sh   1375	1480 1475 1464  1447  1428 1377	  1463    1404 1376	  1464  1445  1420  1377
$\nu(\text{PyO})+$ $\nu(\text{CO})$	1352	1354	1355	1365	1360	1353	1358
$\delta(\text{CH})_{\text{Py}},$ $\delta(\text{CH})_{\text{Ph}}$ $\delta(\text{CH}_2)$		1304 1290		1294 sh	1305		
$\nu_{\text{s}}(\text{PhO}),$ $\delta(\text{NCH})$	1271	1272	1271	1268	1275	1266	1266
$\tau(\text{CH}_2),$ $\nu_{\text{as}}(\text{PhO})$	1250	1251 1243	1248 1242	1249	1260 1248 1236	1289 1242 1226	
$\nu(\text{PyO})+$ $\nu(\text{CO})$	1197	1215	1215	1216	1218	1194	1213



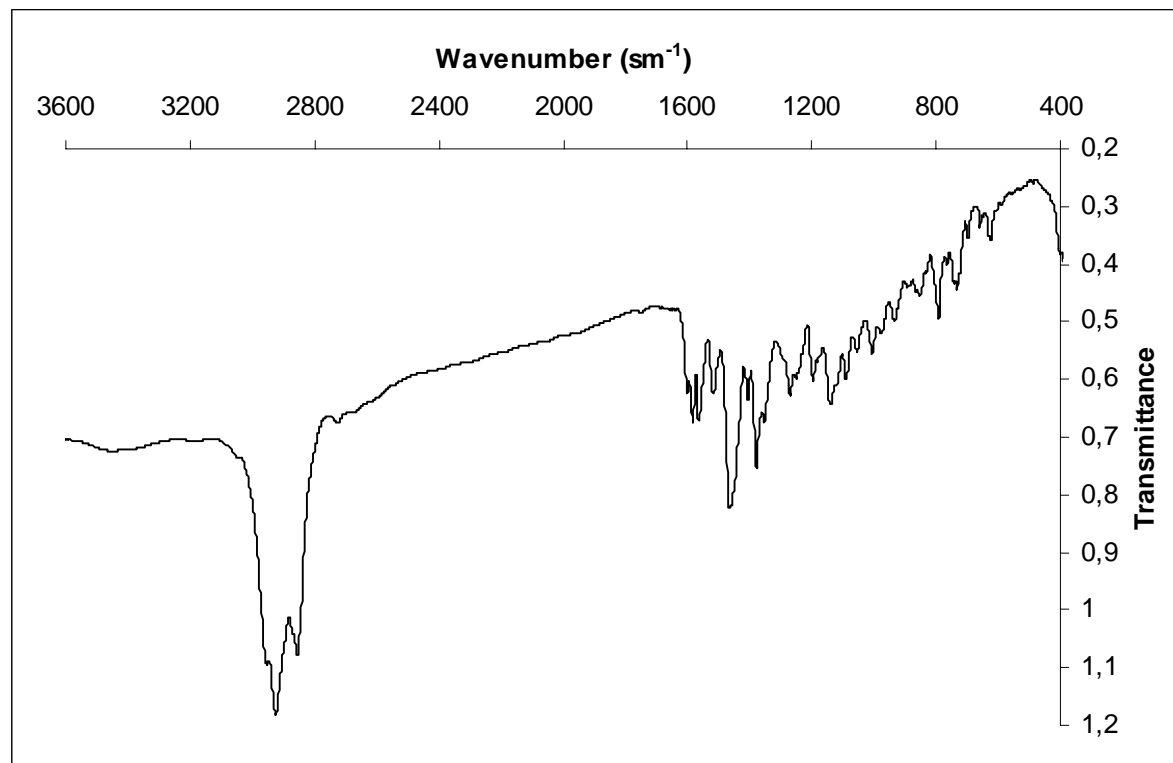
$\delta(\text{CH})_{\text{Ph}}$	1177	1179 1163	1182 1164	1166	1176 1165 1159	1169	
$\delta(\text{CH}_2)^+$ $\nu(\text{CO})$	1144	1138	1138	1135	1129	1124	1135
$\nu_{\text{as}}(\text{COC}),$  $\nu(\text{ClO}_4)$	1119	1119 1112	1118 1111 1100	1106	1129  1095	1101	
$\nu(\text{CO})^+$ $\nu(\text{CC})$	1087  1055  1030	1079 1053 1026	1077 1052 1030	1075 1055 1041 1032	1085 1073 1052 1037 1026	1032	1080   1029
$\delta(\text{CH})_{\text{Ph}},$	1003		1015	1014	1012	1018	1017
$\nu(\text{CH})_{\text{Py}},$	982 975	990 973	991 971	991 978	993 972	989	984 976
$\nu_{\text{s}}(\text{COC})^+$ $\nu(\text{CC})^+$ $\rho(\text{CH}_2)$	953 932 920  890	933 933 910	936	937  904	953 942 911 901 890	968 943 913	935  889
$\rho(\text{CH}_2)^+$ $\nu(\text{CO}),$ $\nu(\text{PF}_6)$	870 855 845 828	875 846 833 814	876 840 811	838	874 868 839	865 835	847
$\nu_{\text{resp}},$ $\delta(\text{CH})_{\text{Ph}}^{\text{np}},$ $\delta(\text{CH})_{\text{Py}}^{\text{np}}$	808 791 766	794 794 765	795 766	793	792 764	792	795

	741	747 727	748 727	749 740 sh 728	752 744 727	745 729	750 727
$\delta(\text{CCO})+$	697	701	701	698	699	696	698
$\delta(\text{COC})+$	660	661	660	661	661	660	661
$\delta(\text{NCC}),$	648		642				
$\delta(\text{CCC}),$	630	638	632	629	633		
$\delta(\text{CNC}),$	622					624	628
	607	611	612		613	603	
	589		594		577	594	
$\delta(\text{PF}_6)$		555	558	558	566		
$\delta(\text{NCS})$						2056 2040	2047

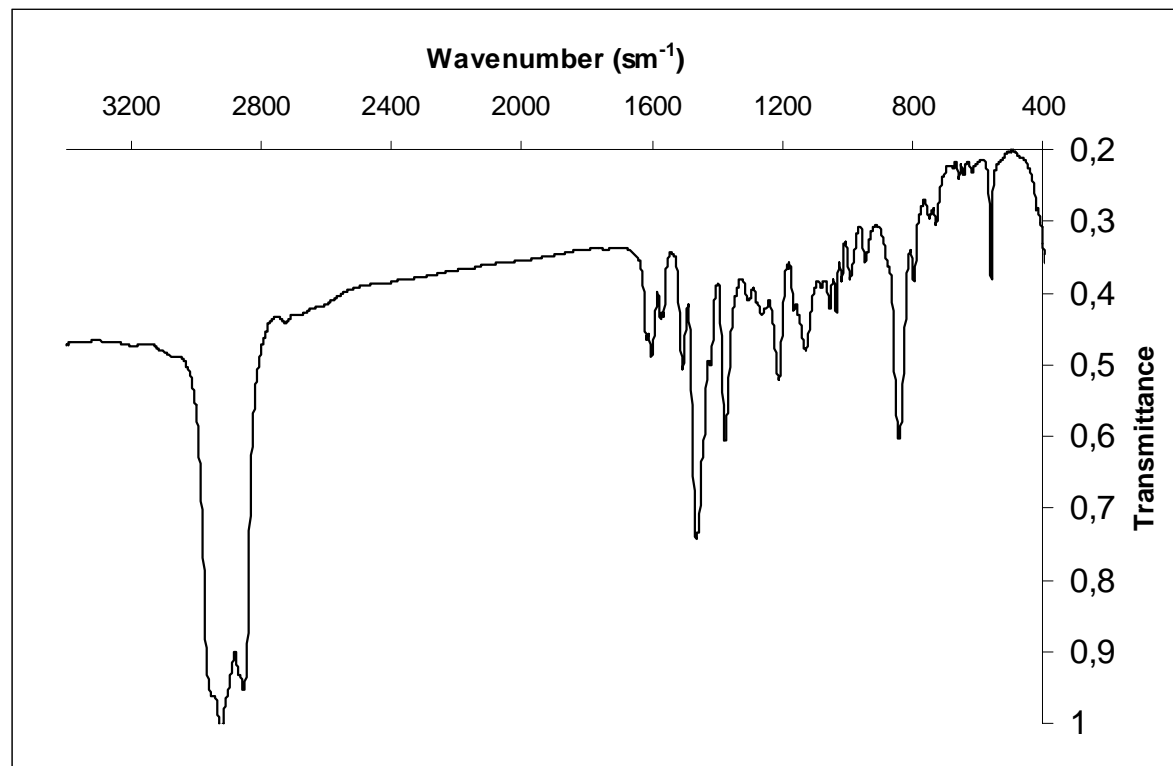
Table 2. Conformationally sensitive vibrational frequencies ( $\text{cm}^{-1}$ ) in the IR spectra of the complexes

Assign- ment	Conforma- tion	L	[NiL <sub>2</sub> ] (PF <sub>6</sub> ) <sub>2</sub> •2(C <sub>2</sub> H <sub>5</sub> OH) •H <sub>2</sub> O (1)	[CoL <sub>2</sub> ] (PF <sub>6</sub> ) <sub>2</sub> •3H <sub>2</sub> O (2)	[CuL <sub>2</sub> ] (PF <sub>6</sub> ) <sub>2</sub> (3)	[ZnL <sub>2</sub> ] (PF <sub>6</sub> ) <sub>2</sub> •3H <sub>2</sub> O (4)	[CoL <sub>2</sub> ] (NCS) <sub>2</sub> (5)	[NaNCS •L]] (6)	[ZnL <sub>2</sub> •2NaNCS] (PF <sub>6</sub> ) <sub>2</sub> (10)	[CuL <sub>2</sub> •2NaNCS] (PF <sub>6</sub> ) <sub>2</sub> (9)	[NiL <sub>2</sub> •2NaNCS] (PF <sub>6</sub> ) <sub>2</sub> (7)	[CoL <sub>2</sub> •2NaNCS] (PF <sub>6</sub> ) <sub>2</sub> (8)
$\nu_{\text{as}}(\text{COC})$	SSG,SSS TGG TGS TGT	1120	1118 1111 1100	1103 1095	1128 1112 1095	1119 1112 1099		1100	1105 1092	1108 1092	1098	1100
$\nu(\text{CO})+$ $\nu(\text{CC})+$ $\rho(\text{CH}_2)$	TGT TGT SGG TGT TGG TST TGG TGG SGG TGS SSG,SSS TGS TGT TST	953 932 920 870 829 855 845	936 912	937 904	953 942 911 901 868	960 933 910	935	943 865 845	937	941	942	941
							858 847					

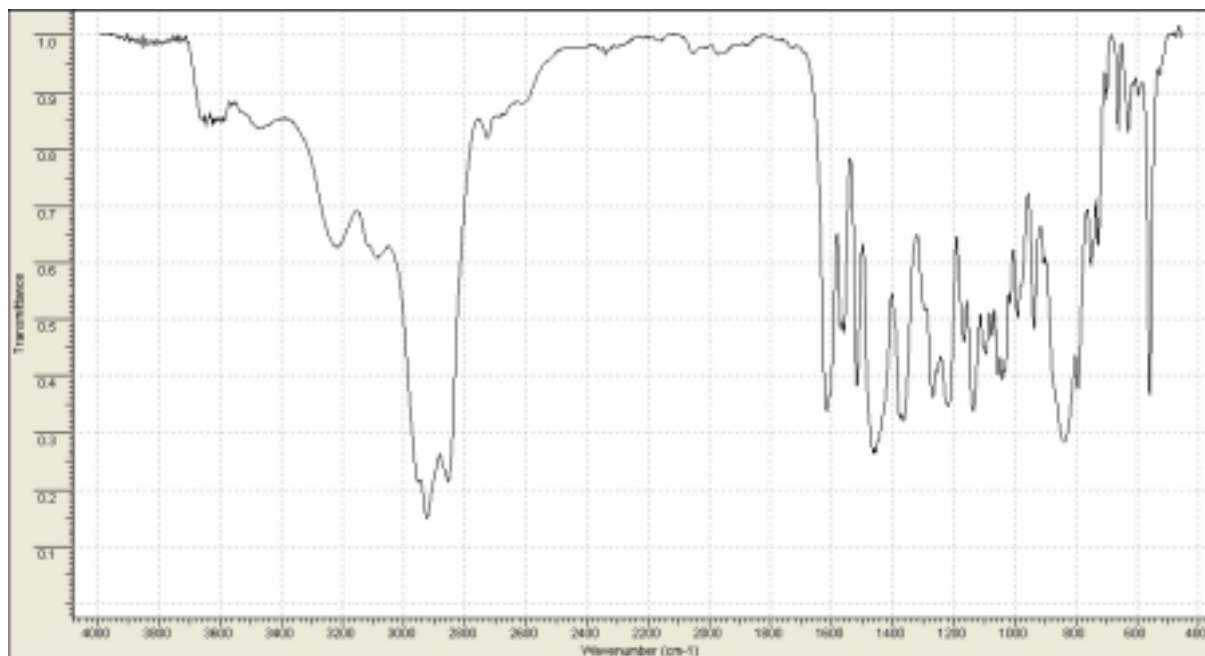
### IR-spectra for *L* and 1-10



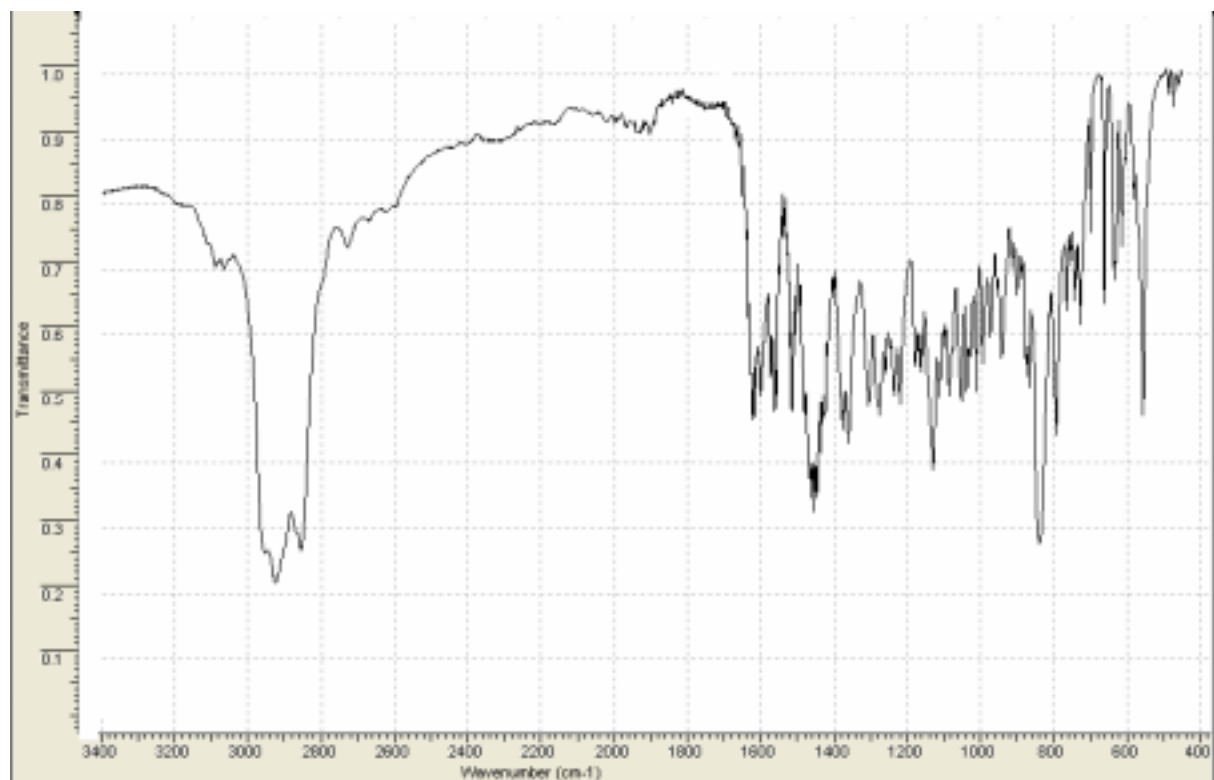
IR spectrum of L



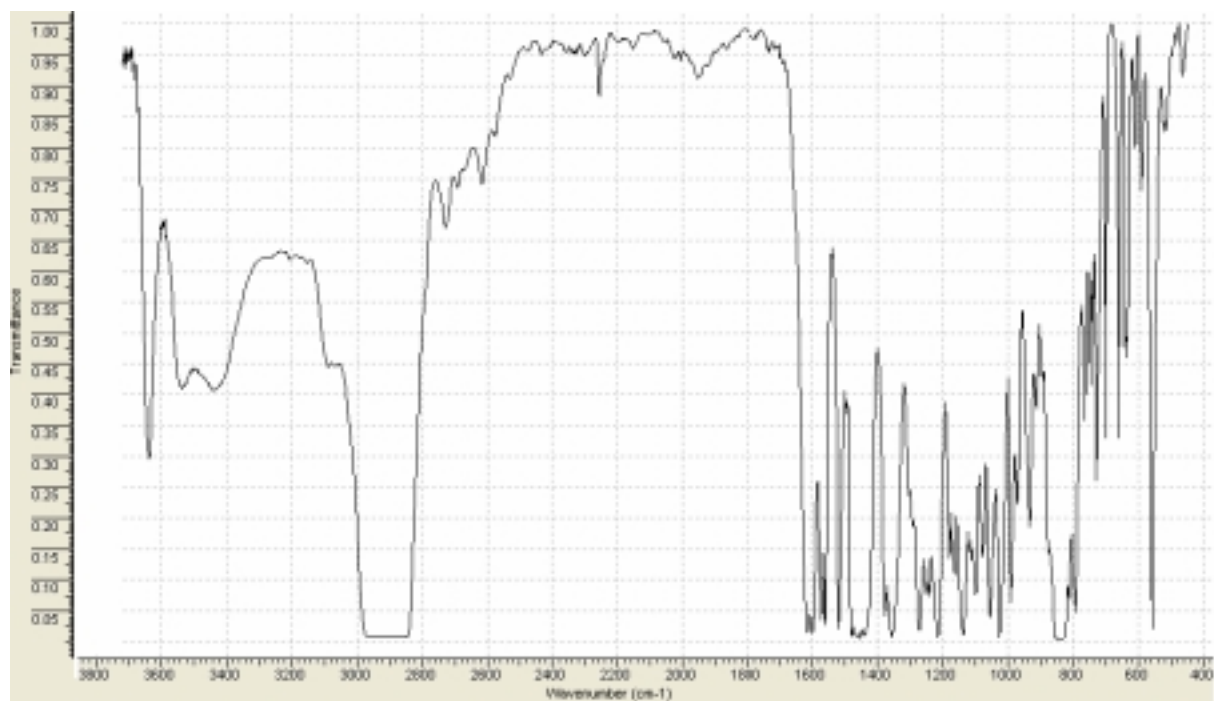
IR spectrum of **1**



IR spectrum of **2**

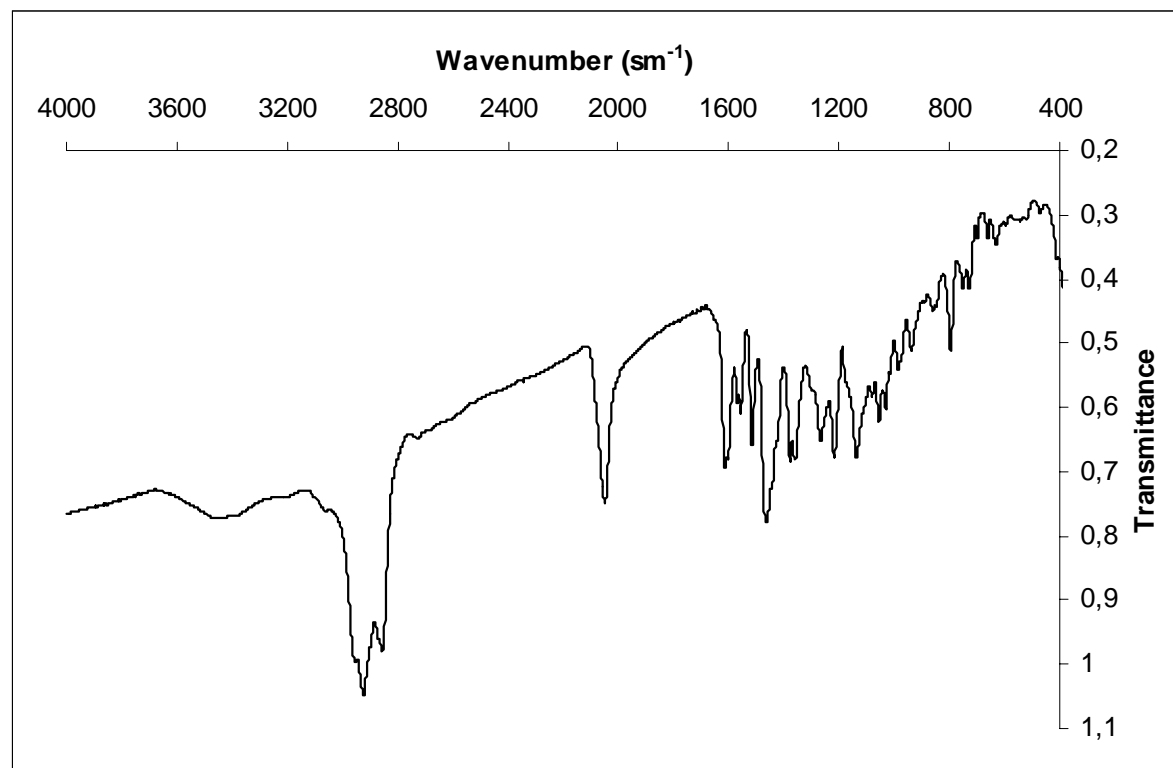


IR spectrum of **3**

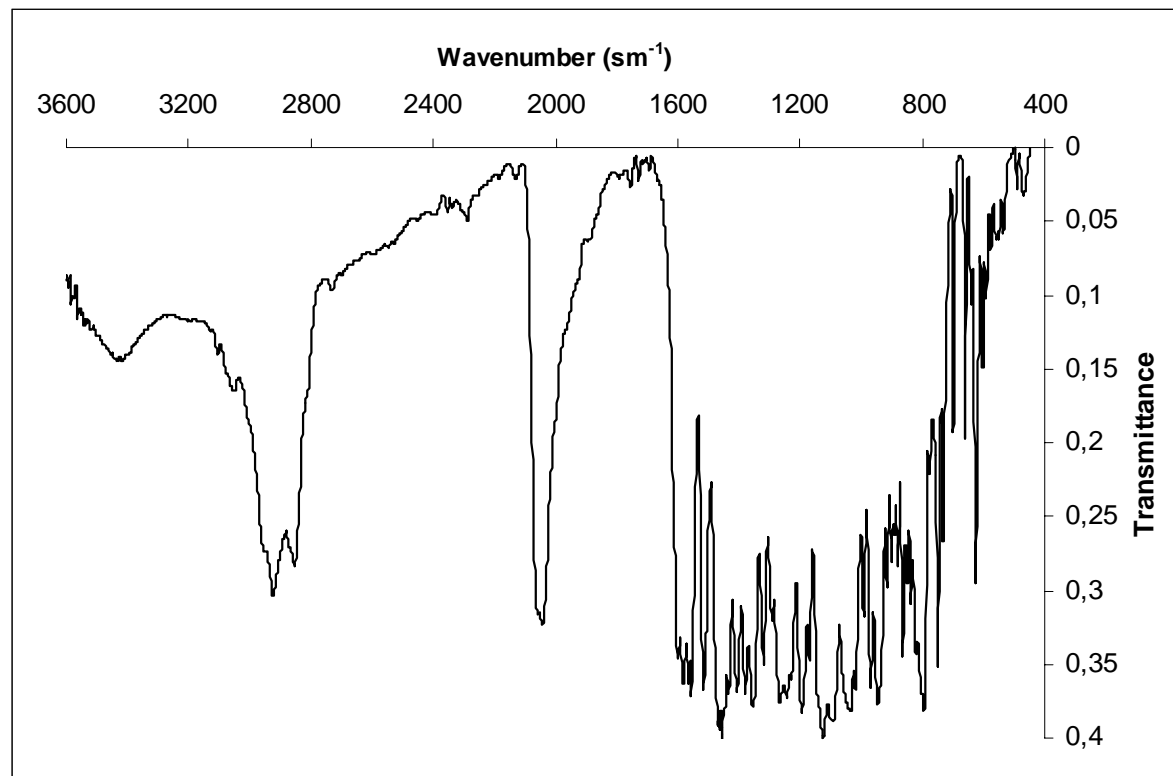


IR spectrum of 4

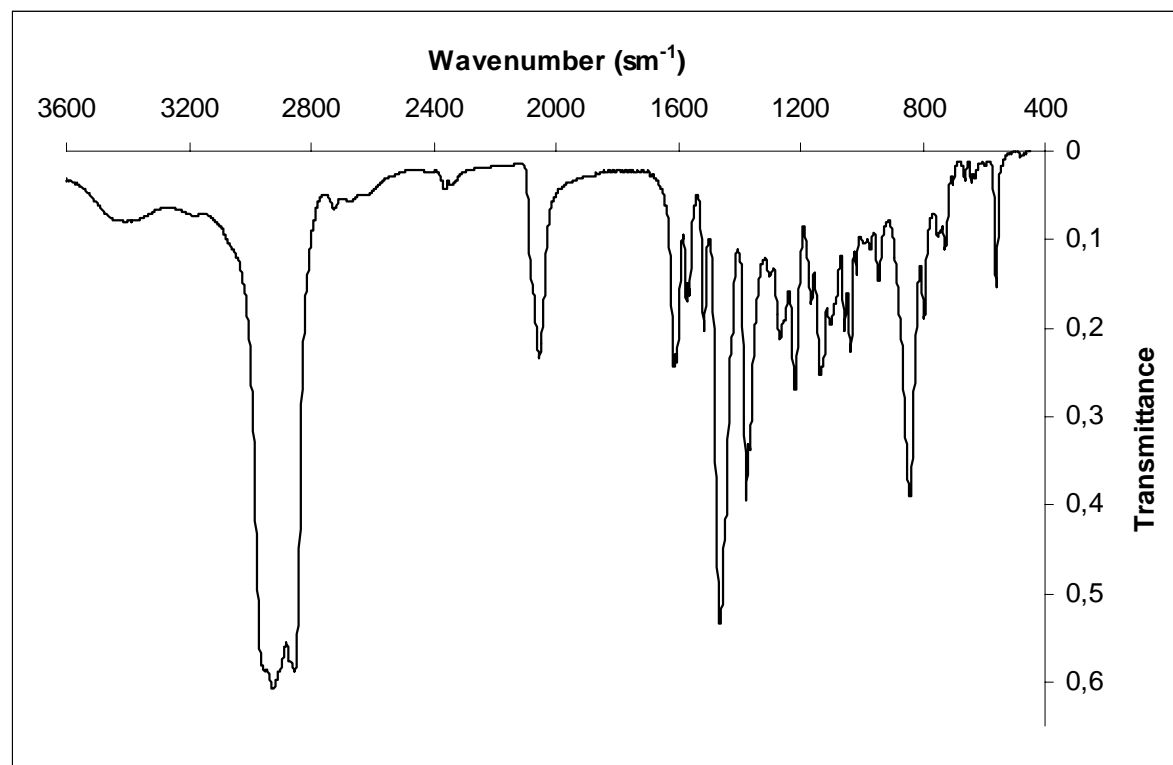




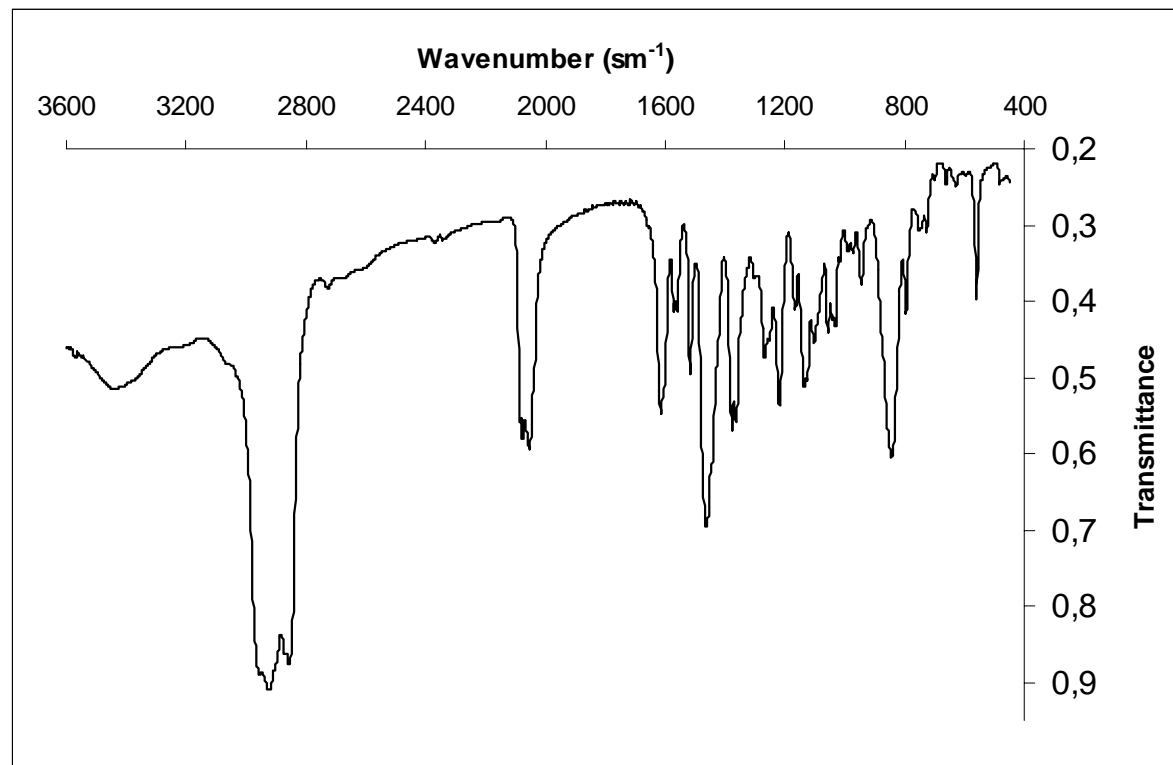
IR spectrum of 5



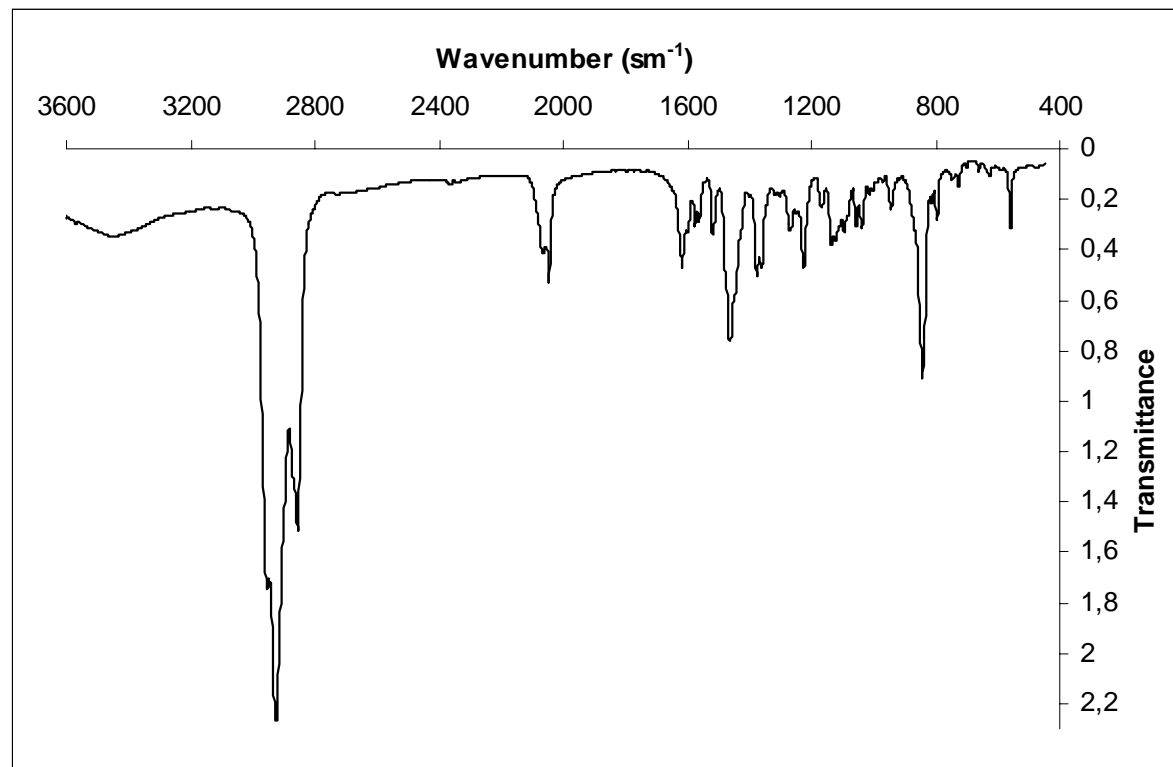
IR spectrum of **6**



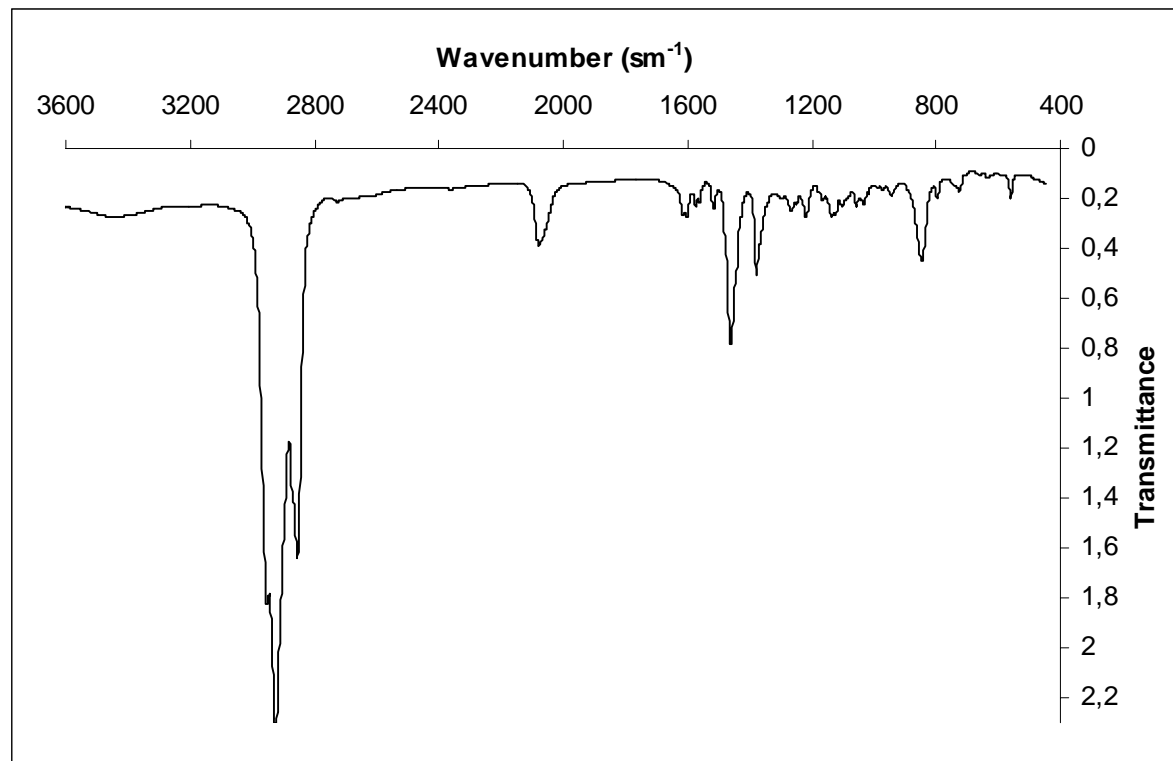
IR spectrum of 7



IR spectrum of **8**



IR spectrum of **9**



IR spectrum of **10**

## PART 2

### X-ray Crystallography. Figures.

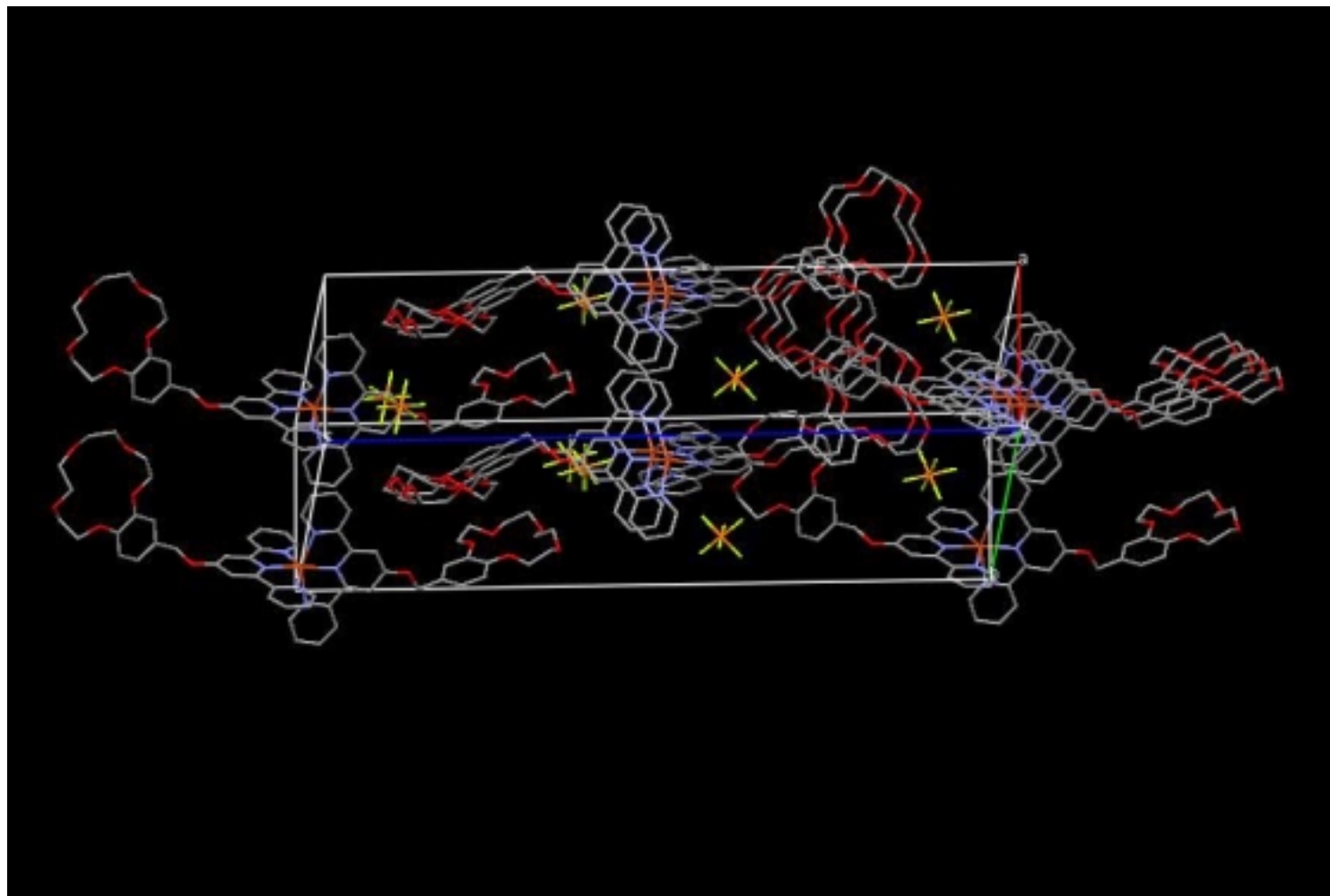


Fig. S2.1 A portion of the crystal packing of **3** showing the unit cell box. H-atoms omitted for clarity.

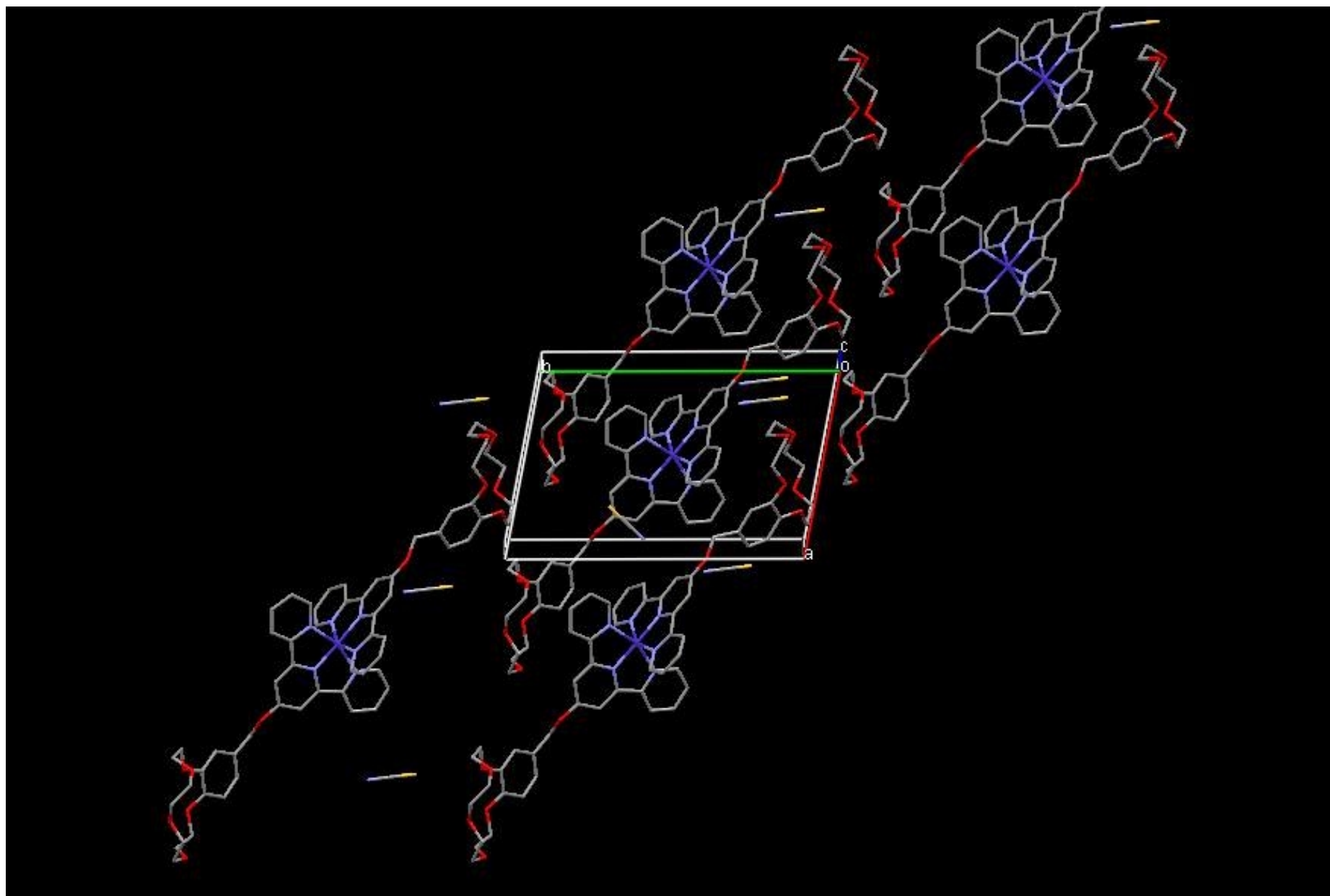


Fig. S2.2. A portion of the crystal packing of **5** showing the unit cell box. H-atoms omitted for clarity.



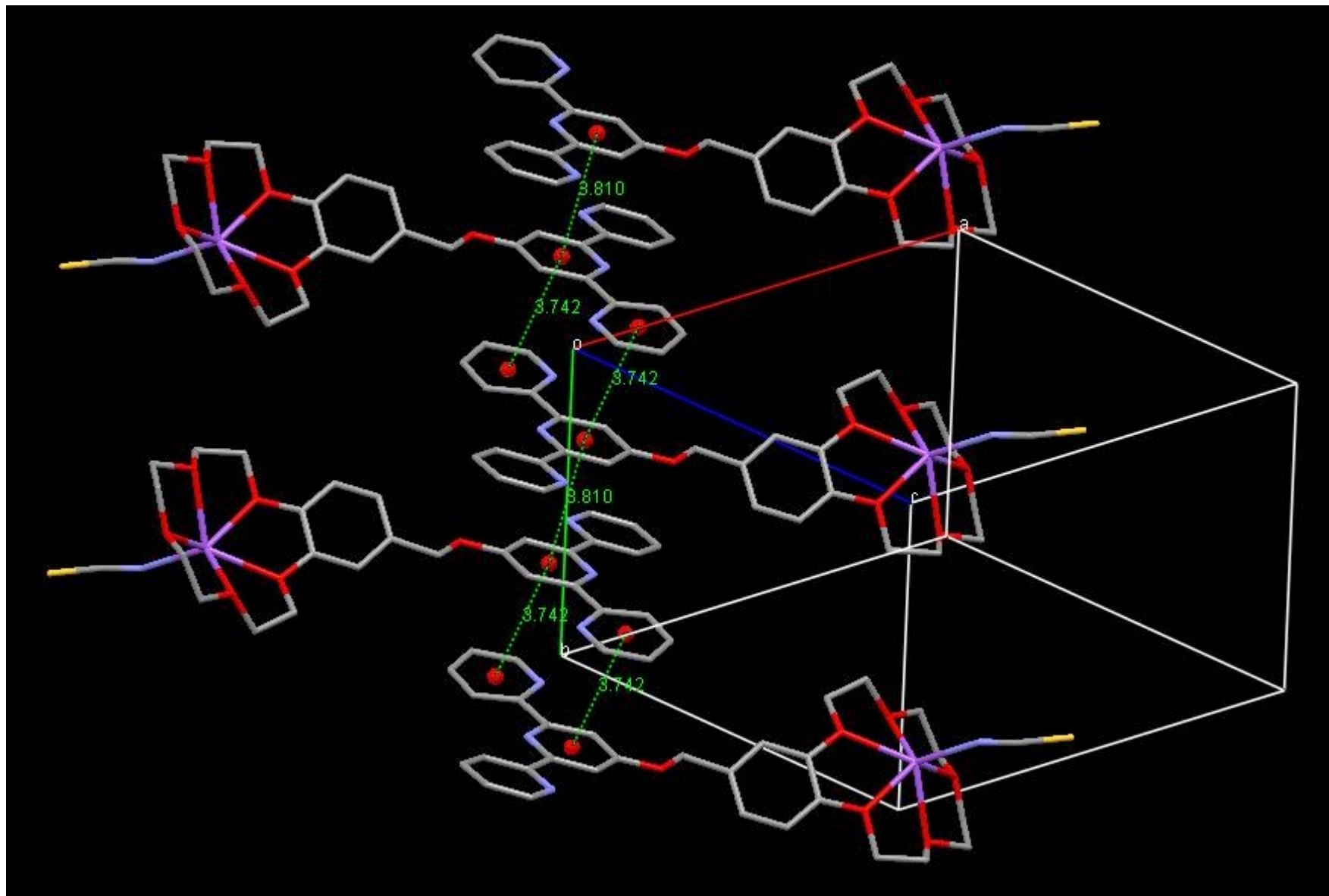


Fig. S2.3. A portion of the crystal packing of **6** showing the  $\pi$ - $\pi$  interactions (dashed lines) in the stacks. H-atoms omitted for clarity.

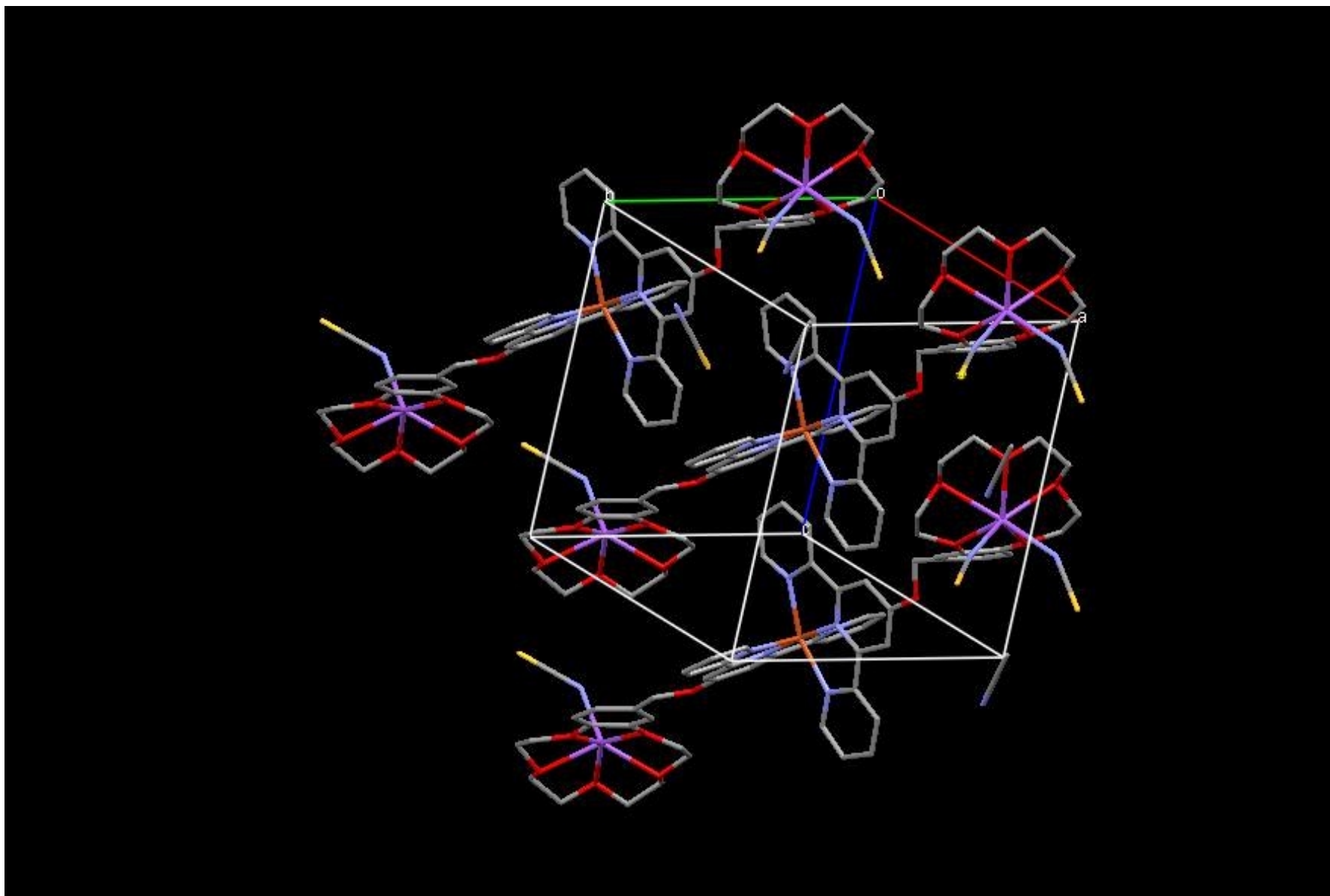


Fig. S2.4. A portion of the crystal packing of **11** showing the unit cell box. H-atoms omitted for clarity.

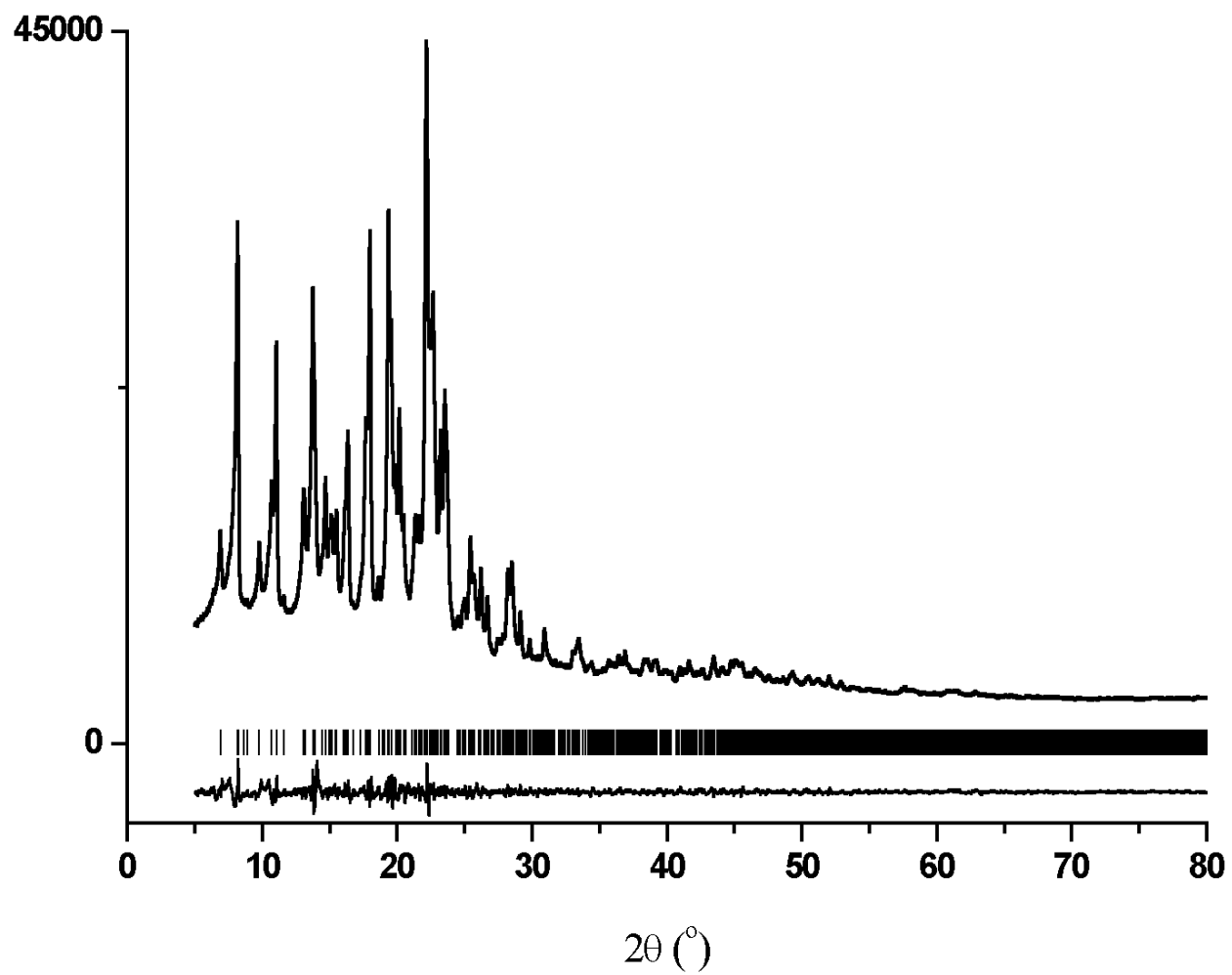


Fig. S2.5 (a) Rietveld plot for **1**.

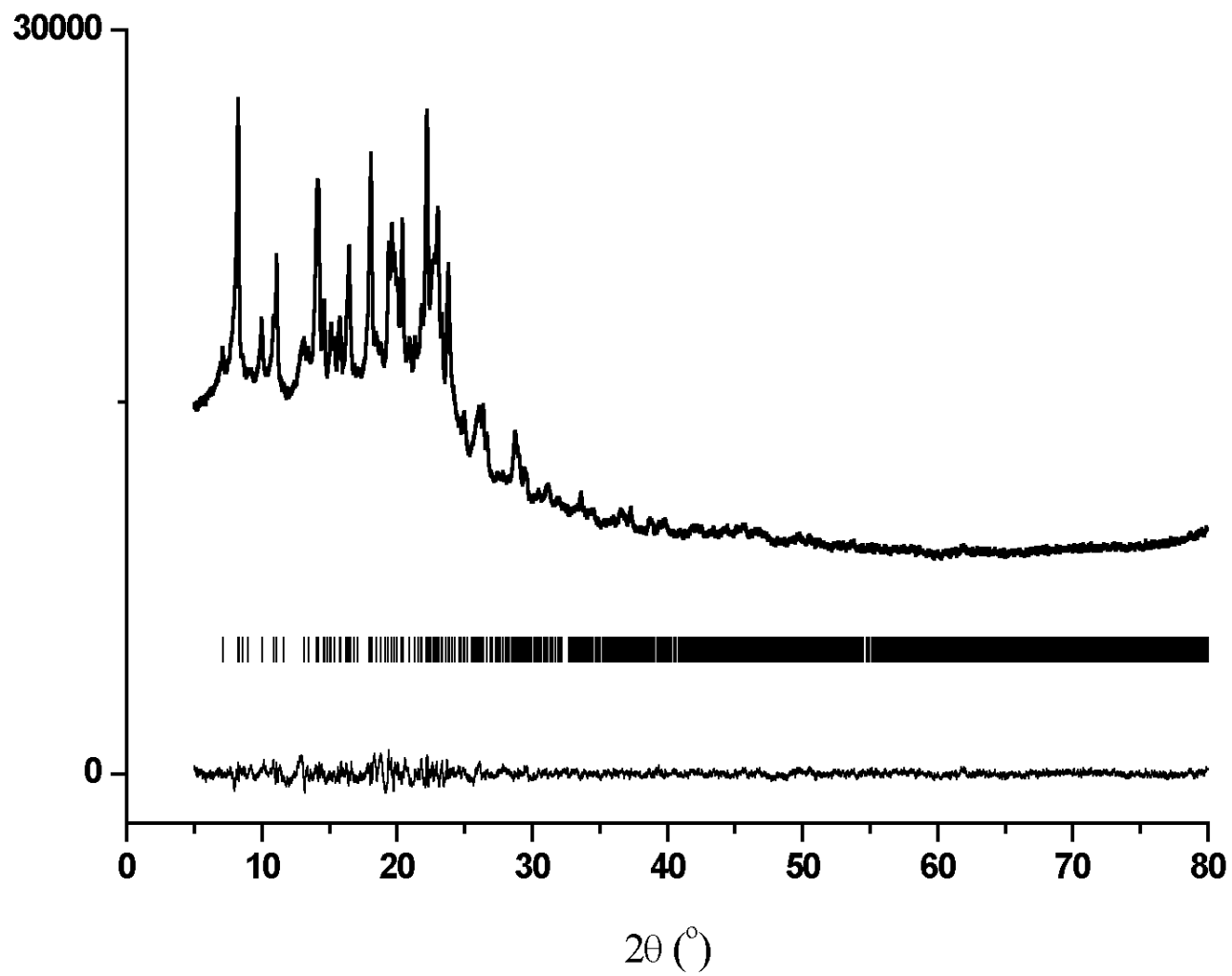


Fig. S2.5 (b) Rietveld plot for 2.

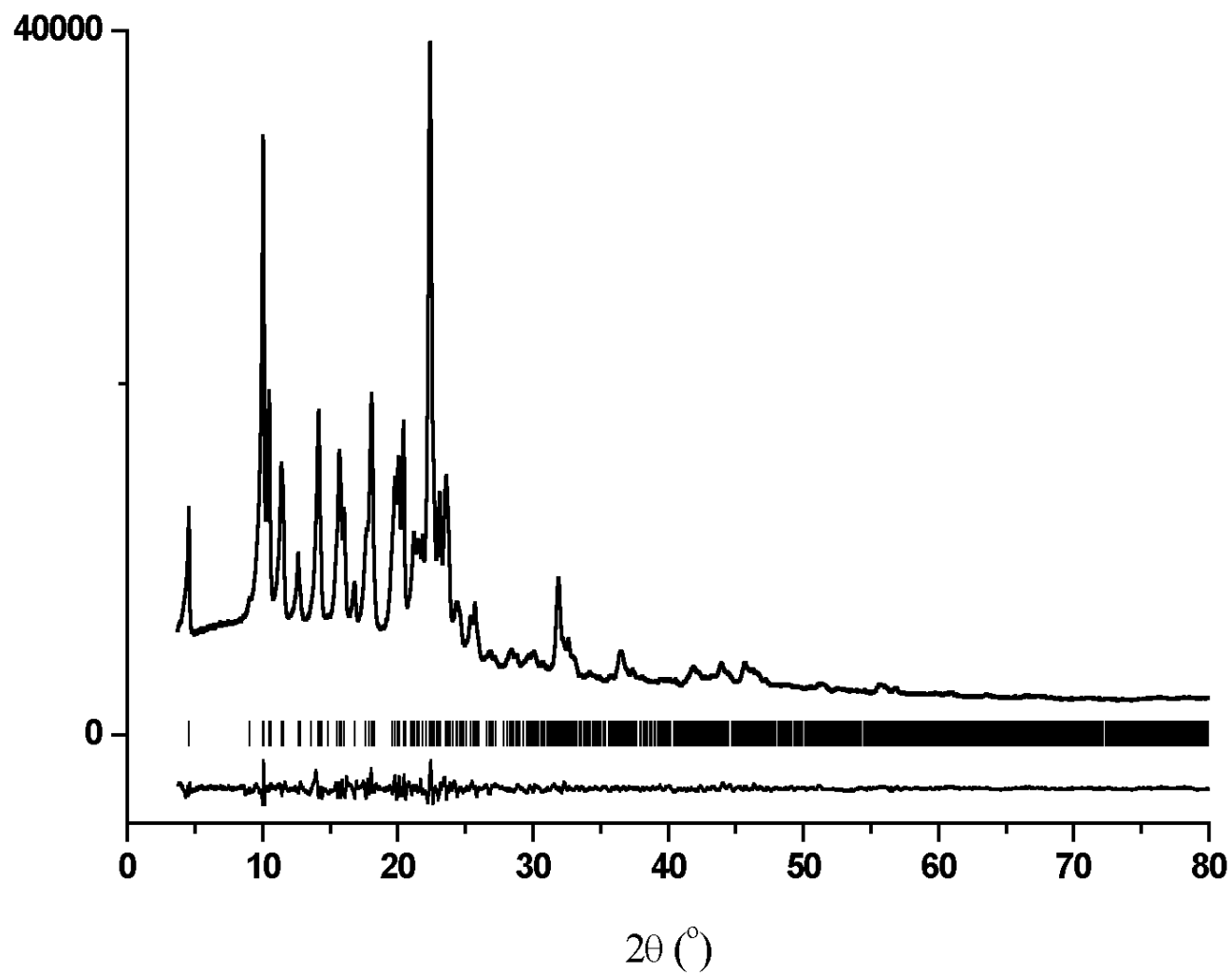


Fig. S2.5 (c) Rietveld plot for 3.

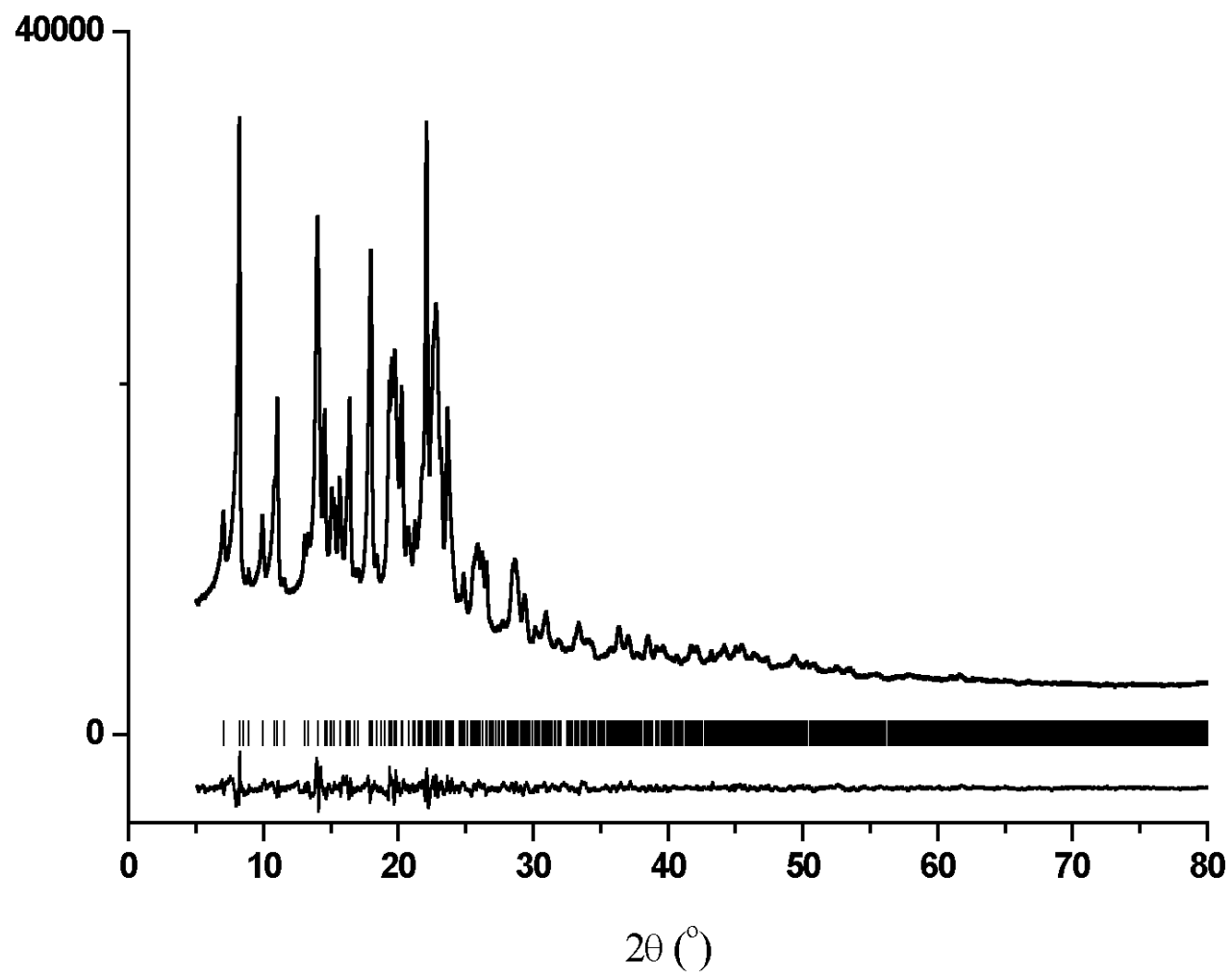


Fig. S2.5 (d) Rietveld plot for 4.

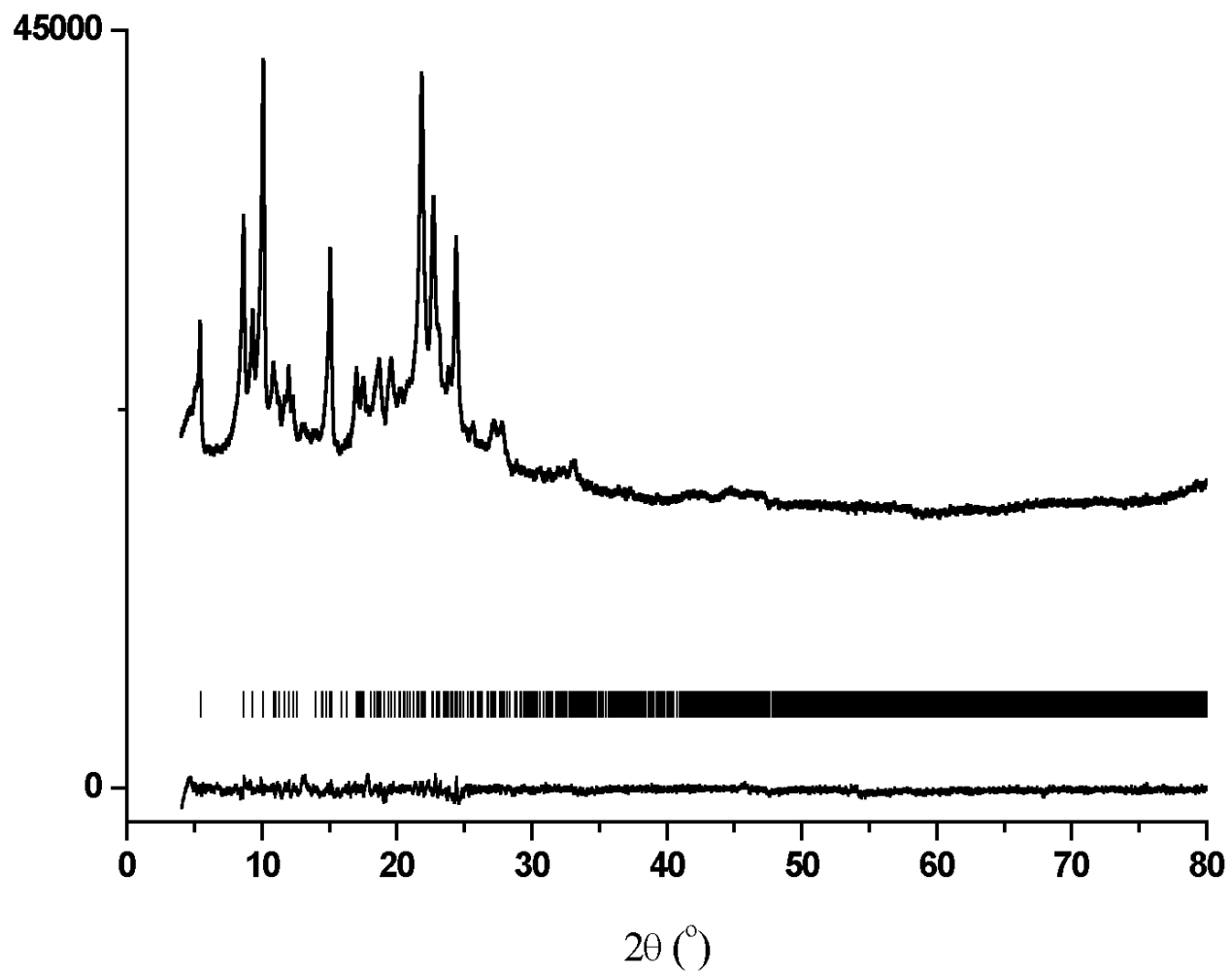


Fig. S2.5 (e) Rietveld plot for 5

